CGMS-48-JMA-WP-08
v1, 7 August 2020

Prepared by JMA
Agenda Item: 4.1
Discussed in Plenary

IMPACTS OF POTENTIAL USAGE OF HYPERSPECTRAL IR SOUNDER ON HIMAWARI-8/9 FOLLOW-ON PROGRAM

In the study reported here, the impacts of hyperspectral sounder installation on a geostationary satellite (GeoHSS) were assessed via observing system simulation experiment to help evaluate the Himawari follow-on program. Hypothetical GeoHSS observations were simulated using an accurate reanalysis dataset for 2018 heavy rainfall and typhoon events in western Japan. The global data assimilation experiment demonstrated that the assimilated GeoHSS clear-sky radiances improved representative meteorological field forecasts and significantly reduced typhoon positional errors. A regional data assimilation experiment showed that assimilated temperature and relative humidity profiles derived from GeoHSS data improved information on heavy rainfall associated with enhanced southwesterly moisture flow off the northwestern coast of Kyushu Island. These results indicate that the GeoHSS provides valuable information on frequently provided data regarding vertically resolved temperature and humidity, thereby helping to improve forecasting of extreme meteorological events.

Action/Recommendation proposed: CGMS agencies are invited 1) to publish and discuss their HSIR OSSE/OSE assessment results for weather/environment applications, 2) to share the information on HSIR such as instrument developments, observation performance, data processing, operation, and applications, and 3) to promote the public awareness of the socioeconomic benefits of the HSIR.

1 Introduction

The Japan Meteorological Agency (JMA) has begun considering a follow-on program for the current Himawari-8/9 geostationary satellites with a view to replacement in FY2029. An infrared hyperspectral sounder (HSS) on a geostationary satellite (hereinafter called GeoHSS) is considered as one of potential payloads for global observation networking as recommended by the Vision for WIGOS in 2040 and for its capacity to help improve JMA's services in relation to extreme weather monitoring, nowcasting and numerical weather prediction (NWP).

This study was conducted to investigate the potential impacts of GeoHSS in the Himawari-8/9 follow-on program based on an observing system simulation experiment (OSSE) using JMA's global and regional data assimilation (DA) systems. Previous and ongoing studies using OSSEs for the GeoHSS have indicated positive impacts on extreme weather prediction (Jones et al. 2017; CGMS-48-NOAA-WP-19), but related research focusing on typhoons and extreme weather in Japan remains insufficient. The present study is expected to help address this situation and provide valuable information for the NWP community and satellite operators, with very few OSSE studies having been carried out using global and regional DA systems. Details of this study (excluding typhoon prediction results) are described in Okamoto et al. (2020).

2 Method

2.1 Reanalysis-based OSSE and GeoHSS simulation

The specifications of the GeoHSS were based on the Infrared Sounder (IRS) on board the Meteosat Third Generation (MTG) satellite. The follow-on satellite is assumed to be at 140.7°E, where Himawari-8/9 are located. Hypothetical GeoHSS observations were simulated using the fifth generation of European Centre for Medium-Range Weather Forecasts (ECMWF) reanalysis (ERA5) data as pseudo-truth atmospheric profiles. Such hypothetical observations are presumed to be virtually independent from real observations, which are already assimilated in JMA's DA systems, because NWP systems incorporating assimilated observations differ between ECMWF and JMA. Events were carefully selected for optimal OSSEs based on hypothetical observation, with ERA5 analysis and subsequent forecasts expected to be more accurate than those derived from JMA's operational system. Hypothetical brightness temperature (BT) data from the GeoHSS were created using Radiative Transfer for TOVS (RTTOV) version 12.2 for all-sky radiances from ERA5 for global DA, and ERA5 grid values for temperature and humidity profiles were bilinearly interpolated for regional DA. The spatial and temporal distances of the hypothetical

GeoHSS were 30 km and 1 h, respectively, as defined in relation to ERA5 products. The coarser spatial resolution than that of the IRS (4 km at nadir) may lead to underestimation of associated GeoHSS impacts, especially for the regional DA system.

2.2 Global data assimilation system

JMA's operational global DA system (GDAS) as of 2018 was used in this study. The system involves the use of an incremental four-dimensional variational (4D-Var) scheme with a horizontal resolution of up to 20 km for the outer model and 55 km for the linearized inner model, and a six-hour assimilation window divided into six time slots. Clear-sky GeoHSS radiances from 36 temperature-sensitive channels and 25 water vapor (WV)-sensitive channels were assimilated in a way similar to that of the HSSs on board the LEO satellites of the operational system, with some modifications. The channel selection was based on the operational HSS setting for temperature channels and Duruisseau et al. (2017) for WV channels. A newly-developed cloud detection scheme effectively identified cloud-contaminated channels when OBTclr – OBT > 1 K for a window channel in which OBTclr and OBT were pseudo-BTs simulated from ERA5 without and with cloud scattering calculation, respectively. The thinning distance was set to 200 km, and samples with large O − B values were removed. Observation errors were estimated from offline calculation of O − B standard deviation and inflated to produce values similar to those of the HSSs on board LEO satellites.

2.3 Regional data assimilation system

JMA's operational regional DA system (RDAS) as of 2018 was used in this study. The system adopts nonhydrostatic 4D-Var scheme, which carries out analysis every three hours by ingesting observations every hour within a 3-h DA window. The horizontal resolutions are 5 km for the outer loop and 15 km for the inner loop, and the vertical resolutions are 48 and 38, respectively, up to 22 km. Significant developments such as bias correction incorporating seasonal changes in carbon dioxide are required for assimilation of GeoHSS radiances because HSSs have not yet been assimilated in the operational RDAS. Accordingly, temperature and relative humidity (RH) profiles thinned to 45-km spacing were assimilated in this study. Thirteen vertical layers (1,000 to 50 hPa) for temperature and seven layers at and below 300 hPa for the RH were chosen for the DA. Data below the highest cloud-affected layer were rejected based on the cloud fraction of ERA5. Observation errors 1.5 times larger than those for the

radiosonde were used in the study. Hypothetical observations exhibiting large O − B values or inconsistencies with surrounding observations were screened out.

2.4 Data assimilation experiment settings and case selection

The extreme rainfall event occurring over western Japan from 28 June to 8 July 2018 was chosen for both the regional and global DA cycle experiments because of the meteorologically important mechanism involved and the requirement to examine the potential for improvement of disaster prevention information. In RDAS, three-hourly DAs for the period from 0000 UTC on 1 July to 0000 UTC on 8 July and 51-hour forecasts for 0000 UTC were carried out. In GDAS, six-hourly DAs for the period from 0000 UTC on 15 June to 1800 on UTC 8 July were executed, and the period of the experiment was extended to early October 2018 for assessment of impacts on typhoon tracks and intensities. The forecast ranges were 264 and 132 hours for 1200 UTC and other initial times, respectively. The impacts of the GeoHSS were compared between the CNT experiment using the operational configuration and the EXP experiment, in which the GeoHSS was added to CNT in both GDAS and RDAS. The RDAS boundary was taken from GDAS.

3 Data assimilation results

3.1 GDAS results

Figures 1a and 1b show hypothetical GeoHSS observations plotted over a six-hour assimilation window. Similar coverage expected to provide valuable information on temperature and humidity was implemented on an hourly basis for the West Pacific region. Figures 2a and b show the relative difference in root mean square errors (RMSEs) between EXP and CNT for temperature and zonal wind forecasts at 72 h. The RMSEs were verified against the initial field of the UK Met Office as an independent reference from ERA5 and GDAS. The figures show that GeoHSS assimilation reduces RMSEs for all altitudes and latitudinal bands, except in northern high latitudes. Zonal wind data is considered to have improved due to the propagation of temperature and humidity enhancement via background error covariance, DA cycle, and 4D-Var tracer advection impacts.

Figure 3a shows averaged errors of 34 track forecasts for typhoon Jebi (1821). EXP shows significantly improved track forecasts; for example, the positional error of four-day (96-hour) forecasts in CNT is equivalent to that of five-day (120-hour) forecasts in EXP. One of the best predictions of EXP, superior to that of CNT, is shown in Figure 3b. Better representation of the large-scale field, as shown in Fig. 2, results

in such an improvement. Here, the weakened western North Pacific subtropical high (WNPSH) in EXP does not prevent Jebi's northward movement.

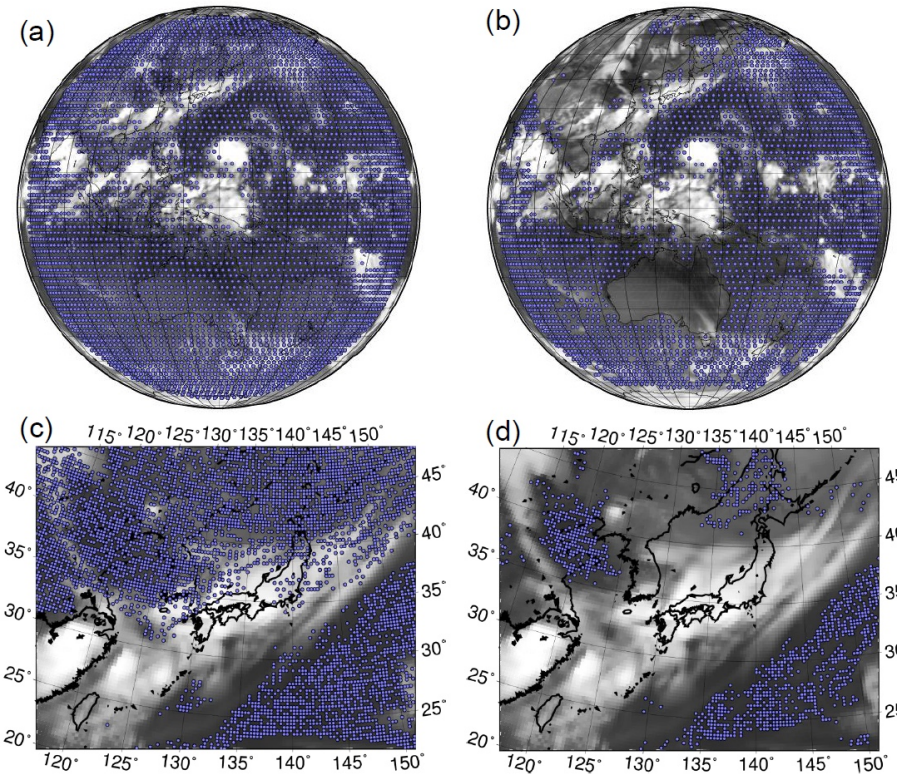

Fig. 1. Hypothetical observations from GeoHSS for (a) channel 3 (14.260 μm, sensitive to temperature at up to 250 hPa) and (b) channel 1400 (5.092 μm, sensitive to humidity at up to 800 hPa) passing quality control (QC) after thinning in the GDAS at 0000 UTC on 6 July 2018. (c) Hypothetical GeoHSS observations of temperature at 150 – 250 hPa and (d) 850 – 1,000 hPa passing QC after thinning in the RDAS. The background monochrome image shows BT simulated from Himawari-8 band 13 (10.4 μm).

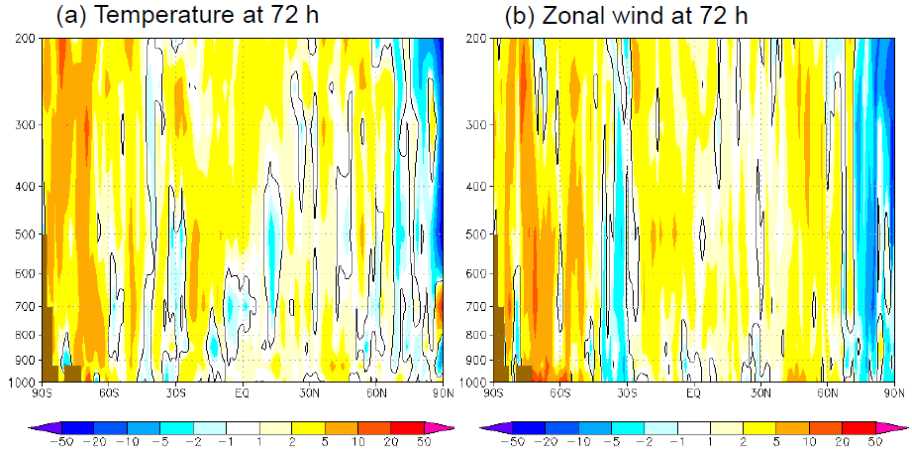

Fig. 2. Zonal mean of average relative difference (%) between EXP and CNT for root mean square errors (RMSEs) verified against the UK Met Office initials for (a) temperature and (b) zonal wind forecasts at 72 h. Positive values indicate RMSE reduction associated with assimilation of GeoHSS radiances.

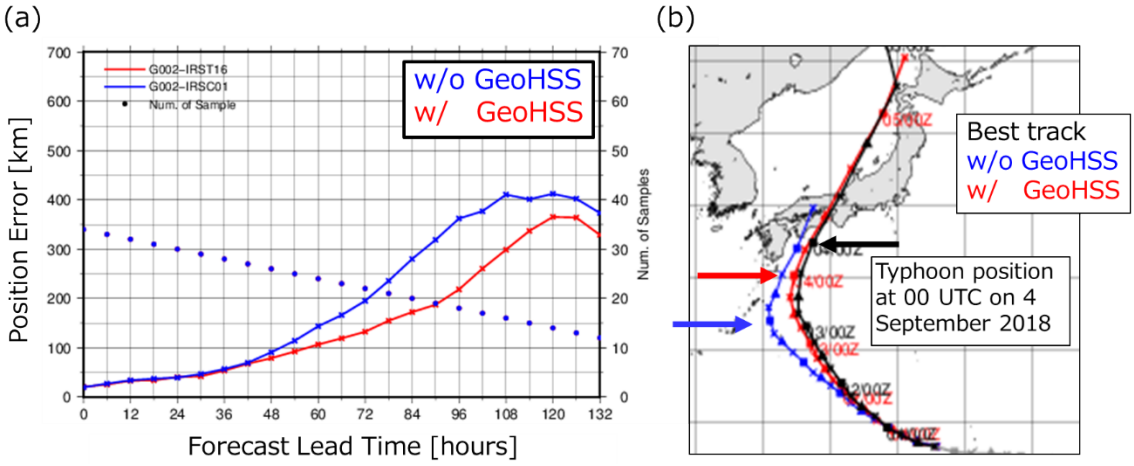

Fig. 3. (a) Track forecast errors for typhoon Jebi (1821) averaged for 34 cases from 12 UTC on 27 August to 18 UTC on 4 September 2018. (b) Typhoon track forecasts for Jebi initiated at 06 UTC on 31 August 2018. Arrows show the predicted typhoon position at 00 UTC on 4 September 2018.

3.2 RDAS results

Figures 1c and 1d show hypothetical GeoHSS temperature observations of for 150 – 250 and 850 – 1,000 hPa after thinning and screening. Again, the dense observations are evident, especially over the ocean and the region upstream of Japan, in contrast to reduced availability at lower altitudes due to cloud screening.

Figure 4 shows verification of initials and forecasts against radiosonde data. Statistically significant improvement of temperature analysis and forecast are observed until 24 h (Fig. 4a). The smaller impacts of GeoHSS in RH (Fig. 4b) suggest significant variability from humidity even after GeoHSS assimilation constraint of RH. As suggested in GDAS, zonal wind data were improved at a significant level in the middle and lower troposphere (Fig. 4c) in association with the propagation of temperature improvements through the background error and DA cycle. Figures 5b and c show the three-hour cumulative rainfall forecast for 21 h initialized at 0000 UTC on 6 July. Both experiments predict heavy rainfall in western Japan well overall, but CNT fails to predict the Chugoku-region rainfall that caused devastating flood conditions. Meanwhile, EXP better predicts rainfall (Fig. 5c). Figures 5d – 7f show the moisture flux difference between EXP and CNT at 850 and 950 hPa. The increased southwesterly moisture flux (indicated by arrows) indicates the major role of strong moisture flux over the ocean. As the northwestern coast of Kyushu Island (west of the Chugoku region) was

covered by frontal clouds (not shown), the intensified moisture flux is probably attributable to the impacts of improved analysis in clear-sky regions reaching the west coast of Kyushu Island in association with the assimilation cycle.

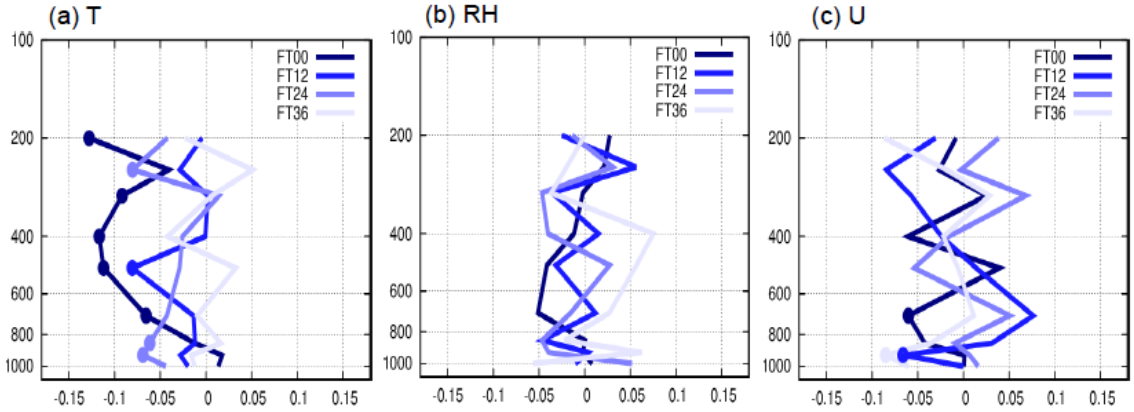

Fig. 4. Relative RMSE differences of EXP and CNT forecasts normalized using the CNT RMSE (($RMSE_{EXP}$- $RMSE_{CNT}$)/$RMSE_{CNT}$) for (a) temperature, (b) relative humidity, and (c) zonal wind at forecast ranges of 0, 12, 24, and 36 h. The RMSE was calculated against radiosondes in the RDAS region, with negatives indicating RMSE reduction or EXP improvement. Dots show statistical significance evaluated based on a 95% confidence interval.

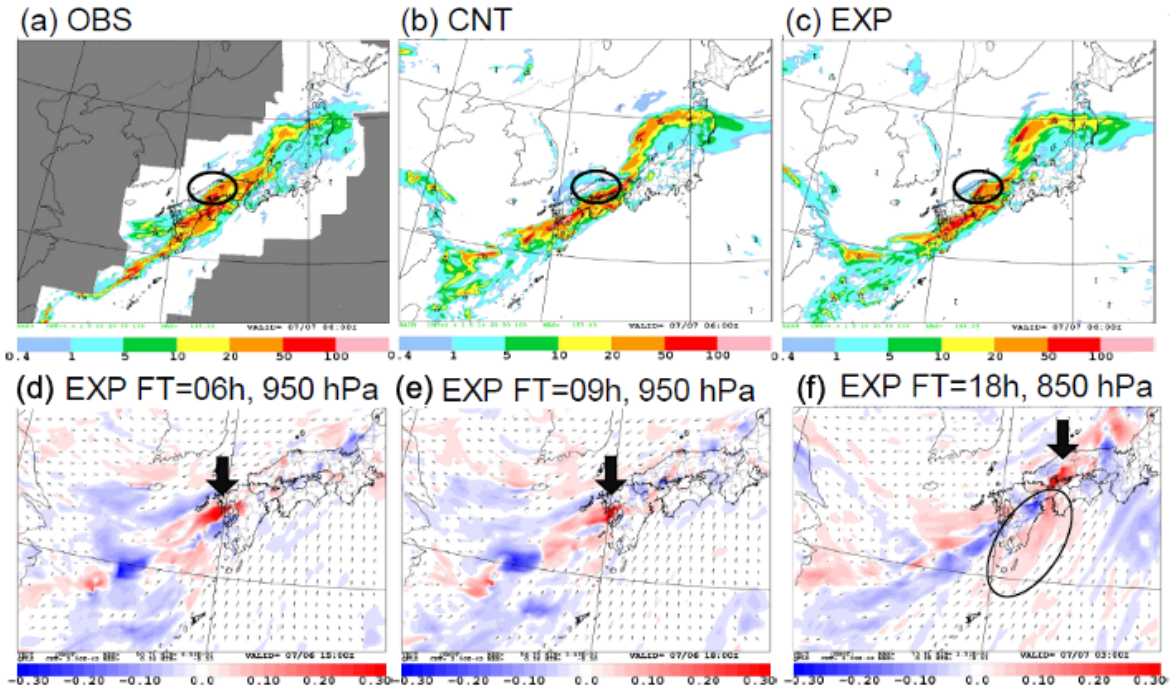

Fig. 5. Three-hour cumulative rainfall (mm) at 0000 UTC on 6 July 2018 from (a) radar/rain-gauge observations made at 21 h in (b) CNT and (c) EXP. Rainfall in the Chugoku region is marked with black circles. (d – f) Difference in moisture flux forecasts (shading, kg m^{-2} s^{-1}) between EXP and CNT with wind (arrows) in EXP. Moisture flux intensification associated with the GeoHSS, as described in the text, is indicated with black arrows and ovals.

4 Conclusion and future studies

In this study, the impacts of GeoHSS data with reanalysis-based OSSE were assessed to evaluate the Himawari follow-on program. Very few researchers had previously performed related examination based on both GDAS and RDAS data. The OSSE utilized ERA5 as a pseudo-truth field to simulate hypothetical GeoHSS observations, and the assimilation experiments clearly demonstrated the value of the GeoHSS for heavy rainfall with respect to improved forecasts of moist airflow and the large-scale system of WNPSH and typhoons. These improvements are attributed to the high frequency of observations over wide regions of Japan and in the Western Pacific. The GeoHSS provides meteorologically essential information on vertically resolved temperature and moisture.

Hypothetical GeoHSS observations were not perturbed in this research because related simulation already included ERA5 analysis errors. However, it is worthwhile to assess the impacts of perturbed observation data in association with instrumental errors because the results suggest appropriate accuracy regarding GeoHSS specifications. Preliminary assimilation experiments with such data indicate smaller but positive impacts. More detailed evaluation of these observations will be carried out in future work.

References

Duruisseau, F., P. Chambon, S. Guedj, V. Guidard, N. Fourrié, F. Taillefer, P. Brousseau, J.-F. Mahfouf and R. Roca, 2017: Investigating the potential benefit to a mesoscale NWP model of a microwave sounder on board a geostationary satellite. *Quart. J. Roy. Meteor. Soc*, 143: 2104-2115. doi:10.1002/qj.3070.

Jones, T. A., S. Koch, and Z. Li, 2017: Assimilating synthetic hyperspectral sounder temperature and humidity retrievals to improve severe weather forecasts, *Atmos. Res.*, 186, 9-25, doi.org/10.1016/j.atmosres.2016.11.004.

NOAA, 2019: OSSEs for Assessment of Hyperspectral Infrared Measurements from Geostationary Orbit in Support of Potential Manifest of a Hyperspectral Radiometric Spectrometer on GEO-XO, CGMS-48 WP-19.

Okamoto, K., H. Owada, T. Fujita, M. Kazumori, M. Otsuka, H. Seko, Y. Ota, N. Uekiyo, H. Ishimoto, M. Hayashi, H. Ishida, A. Ando, M. Takahashi, K. Bessho, and H. Yokota, 2020: Assessment of the potential impact of a hyperspectral infrared sounder on the Himawari follow-on geostationary satellite. *SOLA*, in press.